

# Supporting Information

## UV Curable Stimuli-Responsive Coatings with Antifogging and Oil-Repellent Performances

Jingyang Xu, ‡<sup>a,b</sup> Pengpeng Lu, ‡<sup>a</sup> Li Wang,<sup>b</sup> Yong Fan,<sup>b</sup> Weijun Tian,<sup>a,\*</sup> Jianing Xu,<sup>b</sup>  
Jie Zhao,<sup>a,\*</sup> Luquan Ren,<sup>a</sup> Weihua Ming<sup>c</sup>

<sup>a</sup> Key Laboratory of Bionic Engineering, Ministry of Education, Jilin University,  
Changchun 130022, China

<sup>b</sup> College of Chemistry, Jilin University, Changchun 130022, China

<sup>c</sup> Department of Chemistry and Biochemistry, Georgia Southern University, Stat  
esboro, Georgia 30460, United States

\*Corresponding author

Email: [tianweijun@jlu.edu.cn](mailto:tianweijun@jlu.edu.cn) (W. Tian)

Email: [jiezhao@jlu.edu.cn](mailto:jiezhao@jlu.edu.cn) (J. Zhao)

## **Table of Contents**

### **Thickness of the Coatings**

**Figure. S1** SEM images of the cross-sections for as-prepared coatings.

### **Preparation of Terpolymer Poly(AA-co-TFOA-co-BPA)**

**Figure. S2** GPC retention curves of the T-5 terpolymer

**Figure. S3** ATR-FTIR spectra of (a) AA, TFOA, and BPA (b) C-2, C-3, C-5, C-7 and C-9 coating.

**Figure. S4**  $^1\text{H}$  NMR spectra of (a) AA, TFOA, and BPA (b) T-5 terpolymer in DMSO- $d_6$ .

### **Transmittance of Coating**

**Figure. S5** Photo image of a school badge on the C-5 coating compared with that on the bare glass, the red dashed lines indicate the boundaries.

### **Multi-base application**

**Figure. S6** Oil-repellent property of the C-5 coating applied on various substrates (the hexadecane was taken as the prove liquids)

### **Adhesion Force and Abrasion Resistance Tests**

**Figure. S7** Cross-cut tape test of the coatings

**Figure. S8** Tensile strength-displacement curve of the coatings

**Figure. S9** Abrasion resistance test

## Thickness of the Coatings

Scanning electron microscopy (SEM, JEOL JSM-IT500A) was used to measure the thickness of the as-prepared coatings by observing the cross-section after liquid nitrogen quenching. As shown in **Figure. S1**, C-2, C-3, C-5, C-7 and C-9 had the similar thicknesses of 706 nm, 588 nm, 647 nm, 800 nm and 824 nm, respectively.

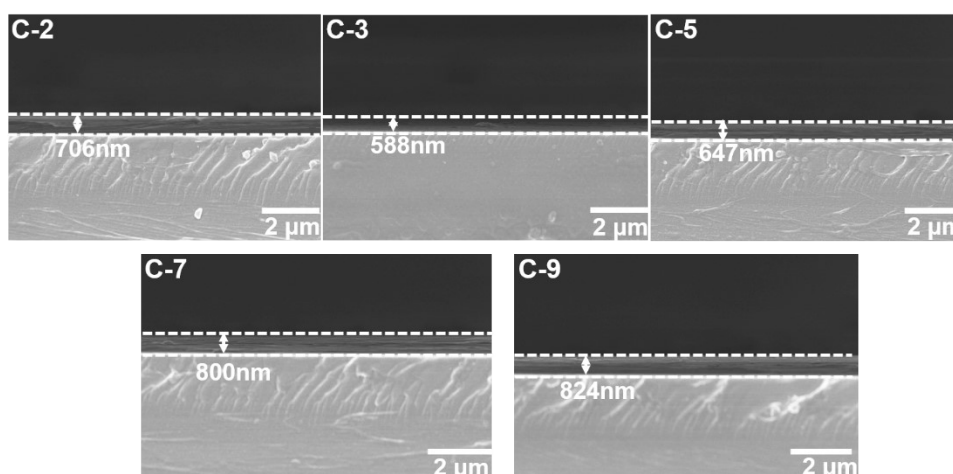


**Figure. S1** SEM images of the cross-sections for as-prepared coatings.

### Preparation of Terpolymer Poly(AA-co-TFOA-co-BPA)

The number-average molecular weight ( $M_n$ ) of terpolymer was measured by gel permeation chromatography (GPC), with a differential refractive index (RI) detector (Waters, 2410), with dimethylformamide (DMF) as the eluent (flow rate 1 mL/min at 80 °C) and polystyrene with the narrow-polydispersity was used as the calibration standard, with  $M_n = 67646$ ,  $M_w/M_n = 1.47$ , as determined from GPC. (**Figure. S2**).

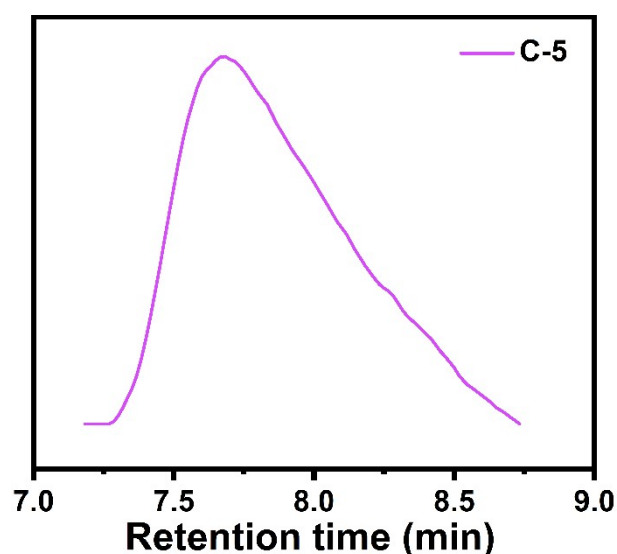


**Figure. S2** GPC retention curves of the T-5 terpolymer.

The structure of the prepared coatings was confirmed by ATR-FTIR spectra as shown in **Figure. S3a**. The characteristic peak at  $3280\text{ cm}^{-1}$  (blue region) was attributed to -OH stretching vibration of the monomer AA, and the  $-\text{CF}_2-$ ,  $-\text{CF}_3$  bending vibration of the TFOA was corresponding to the absorption peak at  $1146\text{-}1240\text{ cm}^{-1}$  (gray region), respectively, revealing that the expected peak also remains in the terpolymers (**Figure. S3b**). We observe that a relative decrease of the =CH- rocking peaks (pink region at  $950\text{ cm}^{-1}$ ), similarly, the intensity of the peak at  $1630\text{-}1695\text{ cm}^{-1}$  (pink regions) which belonged to the  $-\text{C}=\text{C}-$  vibrations became weaker, revealing the copolymerization has

been successfully performed.

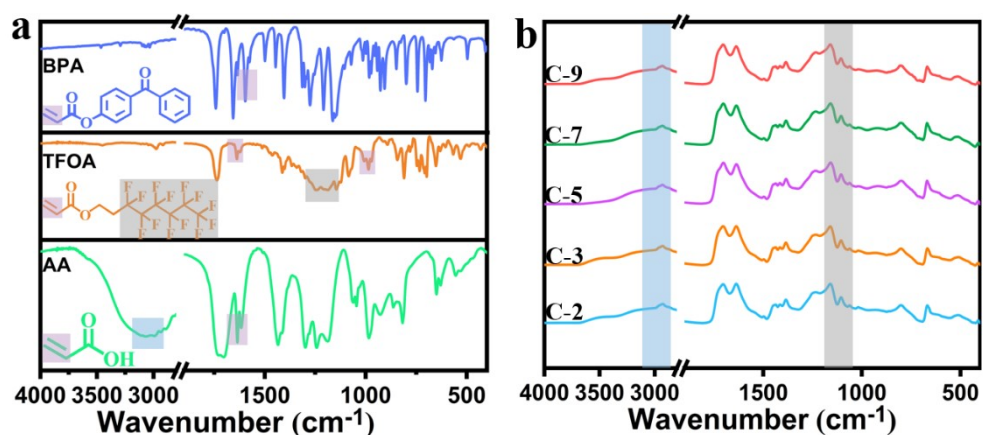


**Figure. S3** ATR-FTIR spectra of (a) AA, TFOA, and BPA (b) C-2, C-3, C-5, C-7 and C-9 coating.

Meanwhile, the detailed chemical composition of poly(AA-*co*-TFOA-*co*-BPA) was further investigated by the  $^1\text{H}$  NMR spectra (**Figure. S4**), the characteristic peak of PAA could be seen at 12.3 ppm (peak a) due to proton of -OH. The proton signal at 4.36 ppm (peak c) originated from the -CH<sub>2</sub>- protons attached to the oxygen in the PTFOA segments. Additionally, the peak at 2.55 ppm (peak d) was a characteristic attributed to -CH<sub>2</sub>- bonding to the perfluorooctyl chain. Signals at 7.5-7.8 ppm (peak b) were derived from the benzene ring protons. The peak of 1.2 - 2.9 ppm (e, f, g, h<sub>1</sub>, h<sub>2</sub>) was assigned to the backbone -CH- and -CH<sub>2</sub>- protons of terpolymer poly(AA-*co*-TFOA-*co*-BPA).

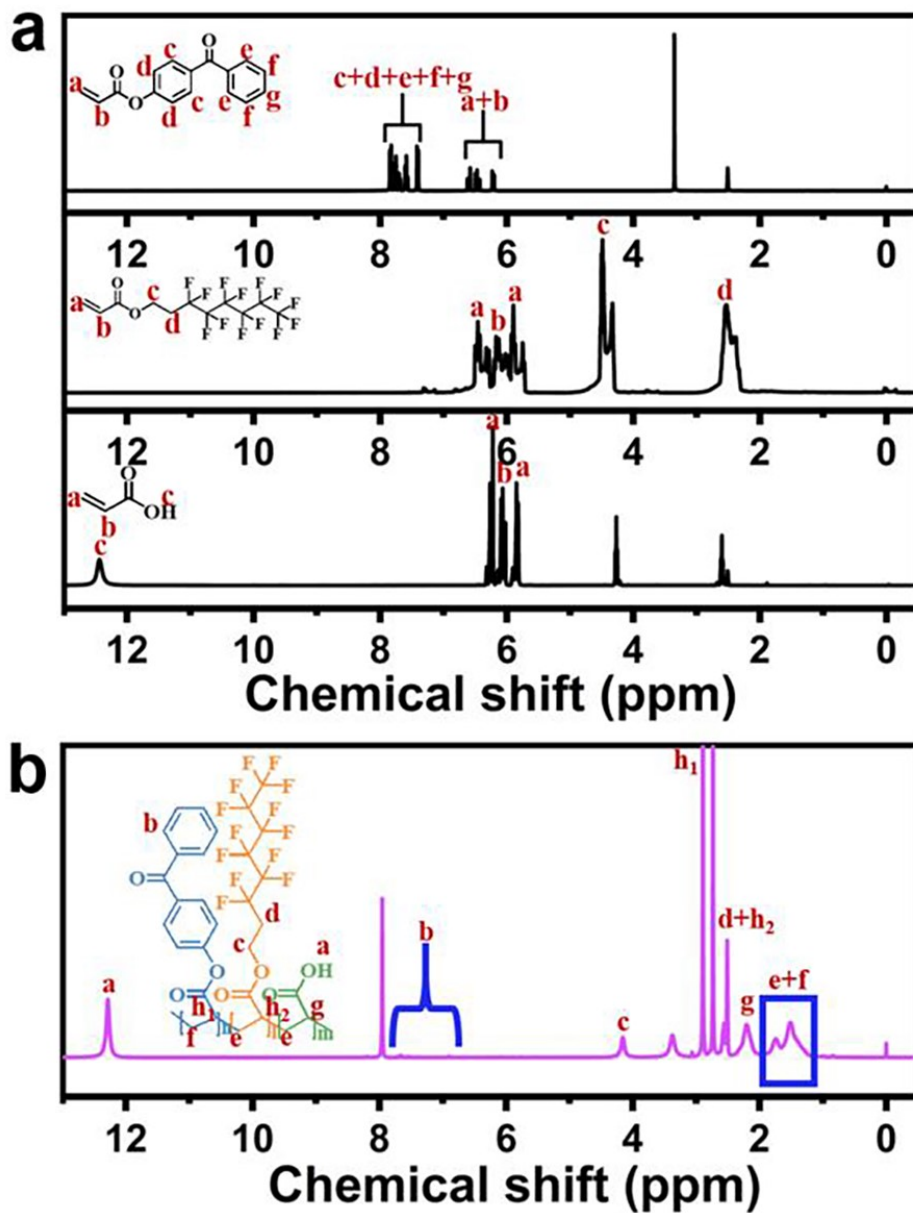


**Figure. S4**  $^1\text{H}$  NMR spectra of (a) AA, TFOA, and BPA (b) T-5 terpolymer in  $\text{DMSO-d}_6$ .

## Transmittance of Coating

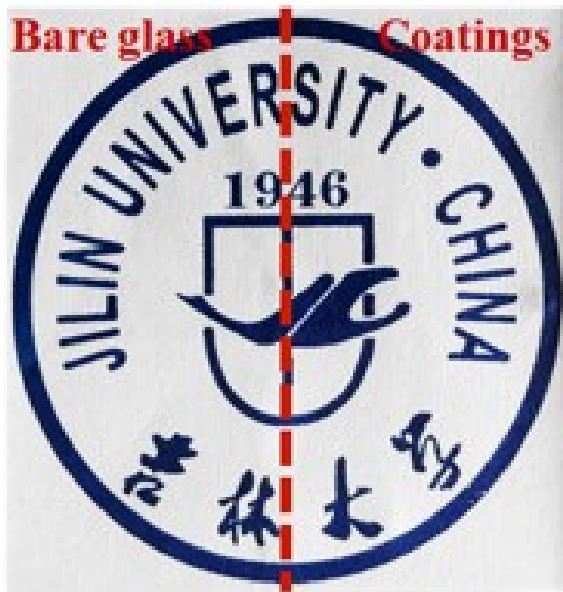


**Figure. S5** Photo image of a school badge on the C-5 coating compared with that on the bare glass, the red dashed lines indicate the boundaries.

### Multi-base application

The applications could occur on the surfaces containing aliphatic C-H groups and apply to various flexible polymer substrates such as glass slide (pre-treated by plasma)

PET, PC, PVC in **Figure. S6**

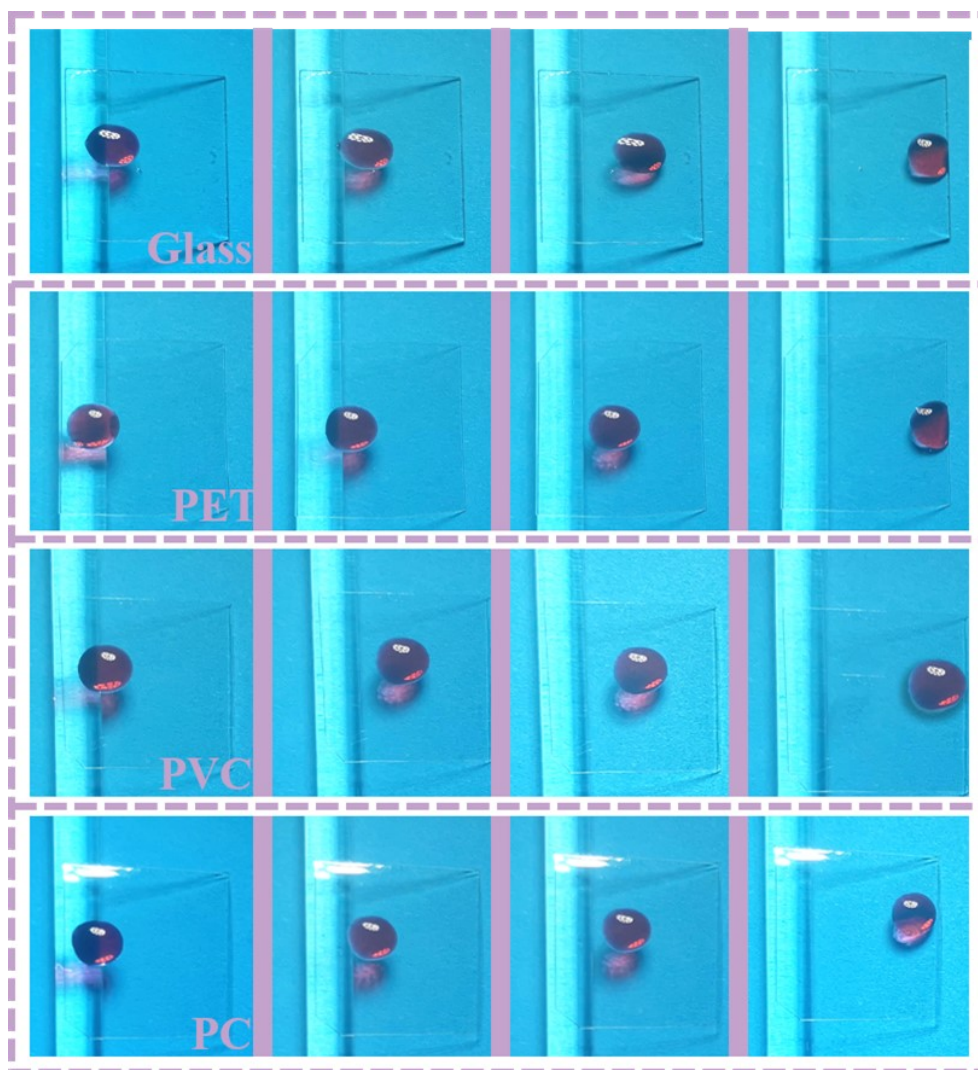


**Figure. S6** Oil-repellent property of the C-5 coating applied on various substrates (the hexadecane was taken as the probe liquid).

## Adhesion Force and Abrasion resistance Tests

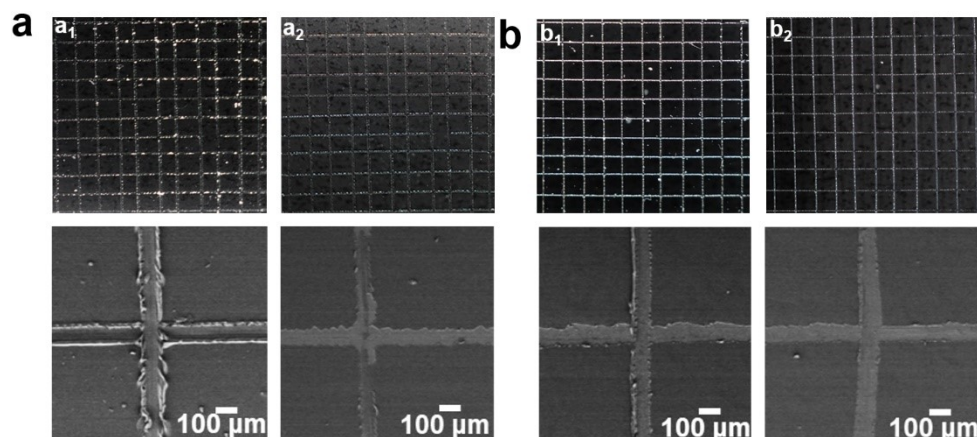


**Figure. S7** Photographs and SEM images of (a) physical deposition coating before (a1) and after (a2) the cross-cut tape test. (b) C-5 coating before (b1) and after (b2) the cross-cut tape test.

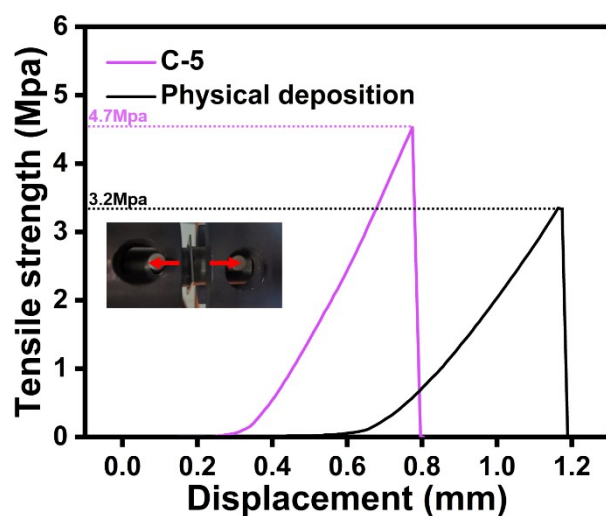


**Figure. S8** Tensile strength-displacement curve of the coatings.

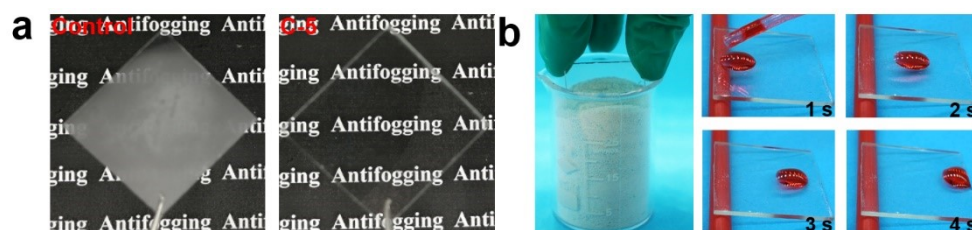


**Figure. S9** (a) Photographs of anti-fog ability after 30 cycles of abrasion test. (b) Photographs of hexadecane sliding off the coating after 30 cycles of abrasion test at a titling angle 10°.

